Environmental Engineering and Management Journal

December 2021, Vol. 20, No. 12, 2033-2048
http://www.eemj.icpm.tuiasi.ro/; http://www.eemj.eu

"Gheorghe Asachi" Technical University of Iasi, Romania

SYNTHESIS AND CHARACTERIZATION OF COMPOSITE MEMBRANE FOR DIALYSIS APPLICATION: ADSORPTION AND RESPONSE SURFACE METHODOLOGY FOR THE REMOVAL OF PHENOL FROM WATER

Naziha Sid-Sahtout[1], Dalila Hank[1,2]*, Amina Hellal[1]

[1]Laboratoire des Sciences et Techniques de l'Environnement, Ecole Nationale Polytechnique, Alger, Algérie
[2]Département Génie Rural, Ecole Nationale Supérieure Agronomique, Alger, Algérie

Abstract

The present study investigates the elaboration and performance of a new Powdered Activated Carbon composite membrane to be used in the elimination of phenol from aqueous solution. The characterization of membranes was determined by Fourier transforms infrared spectroscopy, X-ray diffraction, Thermal gravimetric analysis and Scanning electron microscopy analysis. The effect of treatment, the several parameters such as initial phenol concentration and adsorbent mass have been investigated in batch experiments as well as pH solution on the adsorption process using activated carbon composite membranes. Adsorption isotherm non-linear studies indicate that the Langmuir isotherm provides an adequate fit to the isotherm data. The maximum monolayer adsorption capacity was found 103.08 mg/g. Response surface methodology was used to optimize the adsorption capacity of phenol at equilibrium time and the corresponding operating conditions. The highest adsorption capacity of phenol was theoretically predicted to be 4 mg/g, at which the initial phenol concentration was 20 mg/L, adsorbent dose 0.1 g/L, and agitation speed 250 rpm.

Key words: composite membrane, dialysis, isotherms, powdered activated carbon, response surface methodology

Received: October, 2020; Revised final: April, 2021; Accepted: October, 2021; Published in final edited form: December, 2021

1. Introduction

In water treatment the phenol is worldwide a challenging environmental problem due to rapid industrial development (Ba Mohammed et al., 2019; Mishra et al., 2019). The phenol compounds are found in the environment, through wastewaters, that come from many industrial processes, such as pharmaceuticals, tanning, oil refineries, manufacturing plants, paper making, textiles, and plastic industries (Mandal and Das, 2019). Consequently, several water treatments to remove phenol have been adopted including the most common process which is coagulation and flocculation followed by sedimentation/flotation and filtration adsorption, activated carbon filtration, ion exchange. Membrane filtration techniques such as Donnan dialysis which appears an interesting and more feasible alternative process due to its relative simplicity and low energy requirements (Idris and Yet, 2006). Recent studies on dialysis membranes were mostly concentrated on the characteristics and the properties of different commercial dialysis membranes such as sieving properties, flow misdistribution, diffuse permeability and pore size distribution (Idris and Yet, 2006).

Adsorption is a well-known method for separation equilibrium and is an efficient method for the removal of low concentration organic pollutants from large volumes of potable water, wastewater, and

* Author to whom all correspondence should be addressed: E-mail: dalila.hank@g.enp.edu.dz, nasahtout@gmail.com, amina.hellal@g.enp.edu.dz; Phone: +213 2152 53 01 / 03; Fax: +213 21 52 29 73

aqueous solutions (Mukherjee and De, 2016). It has proved better than other techniques its flexibility, simplicity of design and easy implementation.

Adsorption process has become quite attractive in the depollution of effluents loaded with inorganic or organic pollutants, due to the valorisation of natural materials which are quite abundant and practically costless. In this process, activated carbon is the most used adsorbent for its micro-pores, large surface area, and high adsorption capacity.

Compared with the other separation processes, membrane process have increased its importance by the low energy consumption, easy scale-up, less or no use of chemicals and non-harmful derivate formation (Arthanareeswaran et al., 2008). Membranes can eliminate different pollutants using various processes such as the separation mechanisms of impaction, diffusion, electrostatic interaction, hydrophobic property, and adsorption (Mukherjee and De, 2016). The composites membranes are frequently, in recent years, made by merging organic polymers with different organic or inorganic materials as a probable next generation membrane material (Hwang et al., 2013; Nadour et al., 2019).

The integration of organic/inorganic materials in organic polymers is well-known to increase polymer membranes capacity in permeability, porosity, hydrophobicity and removal efficiency more than those made of single polymers (Arthanareeswaran et al., 2008; Hwang et al., 2013). Previous studies have reported that the preparation of composite membranes by phase inversion method can considerably improve the polymer membranes surfaces morphology and structures (Saljoughi et al., 2009). Phase inversion via immersion precipitation is the most largely applied to prepare asymmetric polymeric membrane (Saljoughi and Mohammadi, 2009). The substrate immersed in a coagulation bath, lead the solvent in the casting solution film to be exchanged with a non-solvent in a precipitation medium and phase separation (Saljoughi and Mohammadi, 2009).

Several studies have examined the combination of organic polymer with inorganic materials like activated carbon (AC), alumina, silica, zirconia, Titania, etc.. Hwang et al. (2013, 2014) works revealed that more the activated carbon (AC) is concentrated, results in bigger pores size, higher porosity of the AC/ polyphenylsulfone (PPSU) /polyetherimide (PEI) / polyethylene glycol (PEG) composite membrane and higher humic acids (HAs) removal efficiency. Similar results were reported for the Cellulose acetate (CA) /SiO_2 via phase inversion process by Arthanareeswaran et al. (2008). Mohamad Said et al. (2017), prepared new organic-inorganic membranes made by uniform Polysufone-Polyethyleneimine-Silver –activated carbon (Psf-PEI-Ag-AC) and observed that AC content reaching 0.9 wt% showed a clear development of sponge structure and has the highest efficiency in elimination of heavy metals. Sid-Sahtout et al. (2020), study revealed the performance of the activated sardine scale powder (ASSP)/ Cellulose acetate (CA)/ Polyvinylpyrrolidone (PVP) and powdered activated carbon (PAC) / Cellulose acetate (CA) / Polyvinylpyrrolidone (PVP) composites membranes prepared by phase inversion in removal efficiency and also exhibits that ASSP /CA/ PVP composite membranes are more porous compared with PAC /CA / PVP composite; this higher porosity leads to more efficiency for the elimination of humic substance in water. The innovative of the present study is the development of a new composite membrane material in order to combine the Powdered Activated Carbon (PAC) adsorption mechanism with the property of separation of the Cellulose Acetate (CA) membrane for the removal of phenol from aqueous solution. The membranes were characterized by FTIR, XRD, TGA and SEM.

Batch experiments were carried out to determine the adsorption isotherms and the effect of various adsorption parameters such as initial phenol concentration, adsorbent mass and pH solution on the adsorption capacity using PAC-membrane. Also, in dialysis treatment the influence of several parameters was studied as initial phenol concentration, adsorbent mass on membrane and agitation speed on phenol removal. The effect of each parameter and their interaction on equilibrium adsorption capacity was determined using the response surface methodology, and a statistical model of the process was developed.

2. Material and methods

Phenol (molecular formula C_6H_6O) was procured from Biochem Chemopharma (molecular weight of 94.11 g/mol, analytical purity of 99.00%) and used for all the adsorption experiments. The polymer used for forming membrane is cellulose acetate (CA) (Sigma-Aldrich, USA), Average Mn ca. 50.000). Polyvinylpyrrolidone (PVP) with an average molecular weight of 10.000 g/mol (Sigma-Aldrich, China) was used as an additive. The 1-Methyl-2-pyrrolidone (NMP) with analytical purity of ≥ 99.0% and molecular weight of 99.13 g/mol was purchased from Sigma-Aldrich (USA) and used as solvent. Distilled water was used as non-solvent agent. Table 1 shows the characteristics of powdered activated carbon (PAC) F400 used in this study sieved to obtain a particle size ≤ 320 μm.

Table 1. Powdered activated carbon characteristics (Hank et al., 2014)

Characteristic	*Value*
Origin	Bituminous oil
Iodine number (mg/g)	1050
Specific surface area (m^2/g)	1050–1200
Function of acid surface (mEq/g)	0.23

2.1. Membranes preparation

The composites membranes were prepared by phase inversion methods proposed by Cheng et al. (1988). At first, different amount of PAC particles at 0, 0.1, 0.2, 0.3, 0.4 and 0.5 g were mixed with NMP

and stirred for 1 h. The blend was sonicated for 1h in order to disperse the particles homogeneously. Then added to the initial mixture of cellulose acetate (1.034 wt%), polyvinylpyrrolidone (PVP, 0.2 wt%).

The solution was stirred continuously for 24h to obtain optimal dispersions of the particles in the polymer solutions, then degassed about 24 hours to remove all air bubbles and kept away from direct light of the sun in order to slow down its aging process. The obtained solution was cast with 300 µm casting knife onto a glass plate, and then immediately immersed in a coagulation bath of distilled water at 25°C to complete the phase separation, where the solvent (NMP) and the non-solvent (distilled water) were exchanged (Sid-Sahtout et al., 2020).

The membranes formed were then transferred to another container containing fresh distilled water to remove excess NMP and PVP. After 24 h, the different membranes were ready to be tested, which take the following names (M0, M1, M2, M3, M4 and M5) corresponding to different mass of the CAP.

2.2. Characterization

The elemental compositions of adsorbents were determined by FTIR, XRD and TGA analysis. The scanning electron microscopic (SEM) analysis was carried out for structural and morphological characteristics of pure and composites membranes.

2.2.1. Fourier transforms infrared spectroscopy (FTIR)

The Fourier transform infrared spectroscopy was used to quantify the abundance of chemical functional groups by a Thermo Scientific Nicolet IS 10 with Thermo Scientific ATR Smart iTR Module, in the range (400–4000 cm^{-1}).

2.2.2. X-ray diffraction (XRD)

The XRD analysis of the samples was carried out on a PANalyticalX'Pert pro diffractometer with a copper anode operating at 45kV and 40 Ma. The program scanned angles (2θ) from 4° to 70° with a step time of 10 s. The system of the XRD uses the principle of reflection of X-rays by crystalline materials.

2.2.3. Thermal gravimetric analysis (TGA)

The tests were realized using NETZSCH (STA 409 PC) type equipment, programmed from 25°C to 550°C with 10°C /min heating rate and under nitrogen atmosphere.

2.2.4. Scanning electron microscopy (SEM)

The morphologies of the various adsorbents were characterized by a JEOL JSM -6360LV scanning electron microscope. The electron beams were sputtered on sample and images of adsorbents on varying resolutions were observed.

2.3. Point zero charge determination

Adsorption phenomena are led by multiple factors, especially electrostatic forces that play an important role. These depend of course on the electrical charge of both the adsorbent material and phenol which comes into contact to be adsorbed, where the determination of the point zero charge pH_{pzc} is essential. The determination of the pH_{pzc} is carried out by bringing 0.5 g of CA/PVP/PAC composite membrane into contact with 10 mL of previously degassed water in order to remove the free CO_2.

The mixture is stirred for 48 h until the pH had stabilized, taking the final pH of the slurry as the pH_{pzc} of the adsorbent. This method of determining the point zero charge has been used with efficient results by Moreno-Castilla et al. (2000).

2.4. Adsorption study

Kinetic adsorption is required to understand phenomenon of adsorption and to define the equilibrium time (Ghaedi et al., 2016). Adsorption experiments were carried out in batch system for phenol removal from water using CA/PVP/PAC composite membrane as an adsorbent.

The phenol adsorption isotherms on CA/PVP/PAC composites membranes were performed at pH 5.5 and at room temperature. The volume of the solution, the mass of the adsorbent, the initial phenol concentration, the contact time, and the stirring speed are respectively: 500 mL, 0.1 g, (5-40 mg/L), 1440 min and 180 rpm.

To determine the concentration of phenol in solution, samples were withdrawn using a syringe then filtered by a 0.45 µm diameter syringe filter and analysed with UV-Vis spectrophotometer (Shimadzu mini 1240) set at 270 nm wavelength. The adsorption capacity expressed by the phenol quantity adsorbed at a time q_t (mg/g) and at equilibrium condition *qe* (mg/g) was calculated according to the Eqs. (1-2):

$$q_t = \frac{(C_0 - C_t)V}{m} \quad (1)$$

$$q_e = \frac{(C_0 - C_e)V}{m} \quad (2)$$

where: C_0 and *Ce* are the initial and the equilibrium phenol concentrations (mg/L), respectively. C_t is the phenol concentration at time (mg/L). *V* is the volume of solution (L), and *m* is the mass of adsorbent (g).

2.5. Study of the adsorption of phenol on the PAC/CA/PVP composite membrane in a dialysis treatment

The tests were performed with a cell which is an assemblage of two identical Plexiglas compartments with 225 mL maximum volume capacity each, separated by a membrane of 9.8 cm^2 effective area (Bensaadi et al., 2014) (Fig. 1). The first one called supply compartment is filled with the solution to be treated. The second one is the receiver compartment that contains the reception solution

(Smail et al., 2013; Sun and Wu, 2014). Each compartment is submitted to stirring during all the experiment at ambient temperature. The same volumes of samples are withdrawn with a graduated pipette from each compartment. The amount of the adsorbed phenol is determined from Eq. (3).

$$q_t = \frac{\left[C_0 - (C_f + C_R)\right]V}{m} \quad (3)$$

where: C_0, C_R and C_f are the phenol initial, receiver and feed concentrations, respectively.

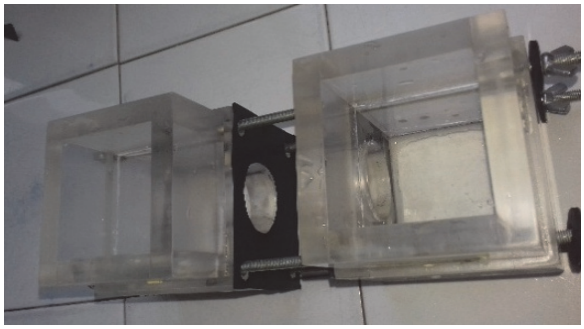

Fig. 1. Transport cell scheme

2.6. Error analysis

The adsorption isotherms parameters of the non-linear models were determined by minimizing the error function and using the solver add-in with Microsoft's spreadsheet, Microsoft Excel. The error function of Chi-square, scale to evaluate the fitting and identify the optimal fit isotherm for the adsorption system, the squared sum of error (SSE) test was calculated to determine the ideal kinetic models fit. The root means square error is a broadly used error function in most of the optimization techniques which aggregate the magnitudes of the errors and is a reliable measure of accuracy and Regression coefficient (R^2) were examined (Karri et al., 2017) as shown in Table 2 (Eqs. 4-7).

3. Results and discussion

3.1. Characterization of membranes

3.1.1. FTIR Characterization

The FTIR has been applied to obtain information about structural and/or physic-chemical properties of the pure CA, PVP, CA/PVP membrane (M0) and CA/PVP /CAP composites membranes (M1, M2, M3, M4 and M5), as shown in Fig. 2 and Fig. 3 (a and b) respectively. It is clear from spectrum Fig. 2 that the principal absorption band of CA which occurs at 1037-1220 and 1737 cm^{-1} is related to the C–O single bond stretching modes and stretching vibrations of the carbonyl group (Xuezhong, 2017), respectively. The main absorption band at 3442-3448cm^{-1}, corresponds to stretching m vibrations of the bulk OH^- ions (Lin and Shiue, 2011).

Moreover, all absorption bands characteristics of CA are present in the FTIR spectra of M0 composite membrane, additionally to the CA absorption peaks (Waheed and Hussain, 2019). A new band was observed at 1648 cm^{-1} that corresponds to carbonyl stretching of PVP due probably to the presence of PVP in the composite membrane matrix (Lin and Shiue, 2011).

The ATR spectra of the CA / PVP / CAP composites membranes are provided in Figs. 3 (a and b). From these Figures, it can be seen that the spectra of the composites membranes with CAP are marked with a new band located around 3662 cm^{-1} characteristic of free elongation vibrations of OH^- (Waheed and Hussain, 2019). The appearance of this new band could probably be the impact of breaking some hydrogen bonds following the infiltration of activated carbon particles between the chains of the two polymers (CA and PVP). A proposed explanatory diagram of this phenomenon is illustrated in Fig. 4.

Table 2. List of non-linear error functions as statistical goodness of fit measures (Karri et al., 2017)

Error function	***Mathematical expression***
Coefficient of determination (R^2)	$R^2 = \frac{\sum_{i=1}^{n}(q_{e,\exp} - \overline{q_{e,model}})_i^2}{\sum_{i=1}^{n}\left[(q_{e,\exp} - \overline{q_{e,model}})_i^2 + (q_{e,\exp} - q_{e,model})_i^2\right]}$ (4)
Sum of the squares of errors (SSE)	$SEE = \sum_{i=1}^{n}\left(q_{e,\exp} - q_{e,model}\right)^2$ (5)
Root means square errors (RMSE)	$RMSE = \sqrt{\frac{1}{n-1}\sum_{i=1}^{n}\left(q_{e,\exp} - q_{e,model}\right)_i^2}$ (6)
Pearson's Chi-square measure	$\chi^2 = \frac{\sum_{i=0}^{n}(q_{e,\exp} - \overline{q_{e,model}})}{q_{e,\exp}}$ (7)
$q_{e,exp}$ and $q_{e,model}$ experimental equilibrium data (mg/g) and theoretically evaluated equilibrium (mg/g) values from the model, respectively.	

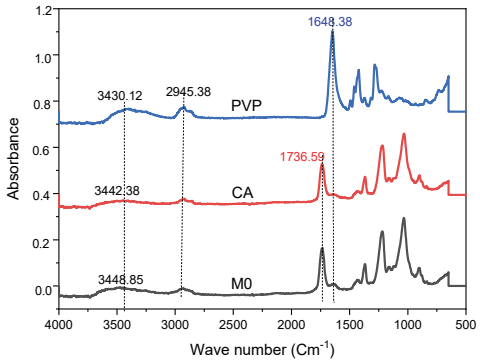

Fig. 2. The FTIR-ATR spectra of CA, PVP and M0 membrane

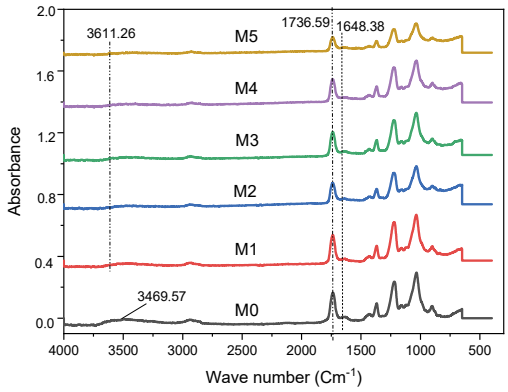

(a)

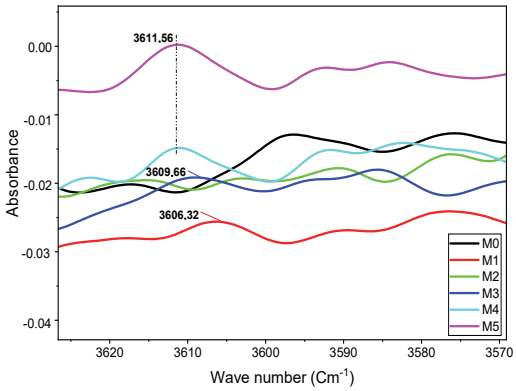

(b)

Fig. 3. The FTIR-ATR spectra of M0 membrane and CA/PVP/PAC composites membranes (a) 4000-450 $cm^{-1}$and (b) 3625-3575 cm^{-1}

3.1.2. XRD analysis

The X-ray diffractogram of the synthesized composites membranes is shown in Fig. 5. All membranes do not give any diffraction. This indicates clearly that the surface of all synthesized membranes is principally amorphous in structures and corresponds to the Van deer Waals halo (Belouadah et al., 2015). Moreover, this amorphous structure of membranes allows us to eliminate the mechanism of ion transfer by successive jumps between agent complexing sites in a 3D assembled state (Zioui et al., 2011).

3.1.3. Thermal stability of membranes

Figs. 6 (a and b) shows the typical thermogravimetric (TG) and its derivative thermographimetric (DTG) curves obtained from the thermal analysis of three composites membranes M2, M4 and M5. From this Figure, it can be seen that these synthetic membranes are degraded in two stages, the first one extends over a temperature range of 250-350°C and corresponds to the thermal degradation of the polymeric chains (Arthanareeswaran et al., 2004).

The second stage starts at 380°C depicts carbonization of the degraded products to ash (Kee and Idris, 2010). In addition, it was found that the weight loss of membranes composite M2, M4 and M5 were 43.05%, 39.36% and 13.02% respectively. It indicated that the presence of different amounts of the inorganic component of PAC can affects the degradation process. It is also noticed that the maximum temperature of the degradation of these membranes is equal to 356, 359, 355°C respectively, and which are found by the first derivative (DTG) the Fig. 6 (b). This result affirms that the synthesized composites membranes indicate a good thermal stability (Abdellaoui and Arous, 2019).

3.1.4. Morphology analysis

The study of the morphology of the membranes prepared with and without PAC was performed on the cross-sections by a scanning electron microscope (SEM), the images are shown in Figs. 7 (a-f), All membranes present a typical asymmetric form with fingers like pores linked (Hassan et al., 2018). This structure is formed as a result of instant demixing produced between the surface of the polymer solution and the non-solvent (water); therefore, the polymer-rich phase forms the thin film that represents the skin of the membrane, and porous structure formation is due to nuclei formation during the polymer-poor phase. The composites membranes containing different CAP compositions Figs. 7 (b - f) show a significant change in the membrane morphology formation, this structure is more porous with more finger-like pores by sponge wall (Moradihamedani and Abdullah, 2017; Sid-Sahtout et al., 2020) than the structure of non- composite CA membrane Fig. 7 (a). The pore distribution (porosity) of the underlay increased with the addition of CAP to the polymer solution (Dehkordi et al., 2015).

3.2. Point zero charge

The pH_{pzc} is a good indicator of the chemical and electronic properties of surface functional groups. When the pH of the solution is lower than the pH_{pzc}, the surface functional groups of the adsorbents will be positively charged, following an excess proton in the solution.

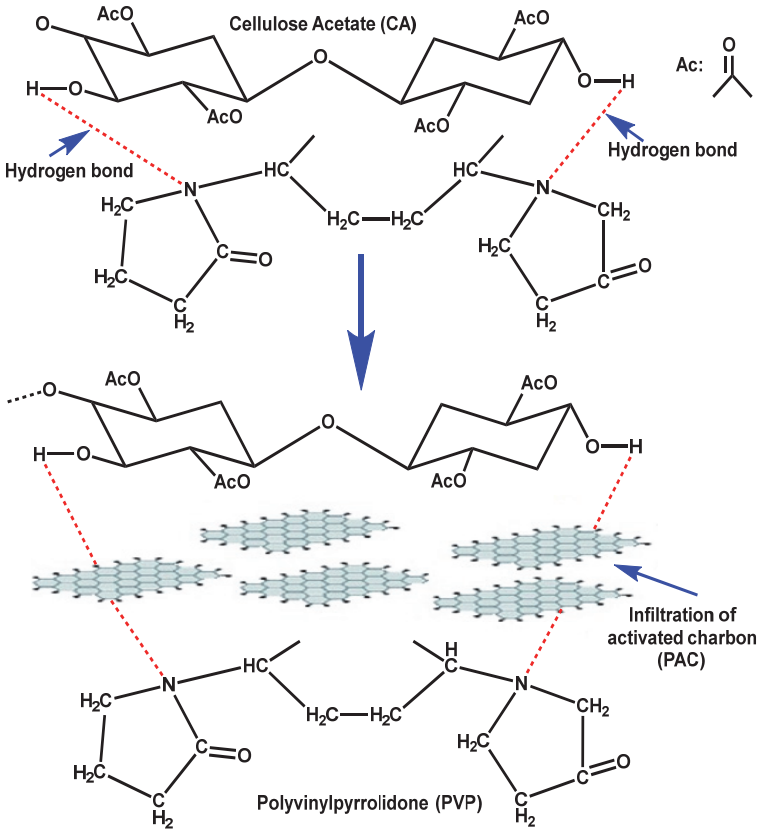

Fig. 4. Explanatory diagrams of the interactions between the constituents of the CA/PVP/PAC composites membranes

While for pH values above pH_{pzc}, the functional groups will be in dissociated form and take on a negative charge which gives the adsorbent a basic character. The adsorbate is principally in protonated form at pH <pKa and in deprotonated form at pH> pKa (Liu et al., 2010).The point zero charge of the adsorbent in this work is 6.15, indicating that the acidic groups are predominant on the surface of the adsorbent.

3.3. Adsorption kinetics

3.3.1. Effect of adsorbent mass

The adsorption of phenol onto CA/PVP/PAC composite membranes was studied by varying the adsorption of phenol onto CA/PVP/PAC composite membranes was studied by varying the adsorbent mass (0.1-0.5 g/500 mL) for the initial phenol concentration of10 mg/L, stirring speed (180 rpm), ambient temperature and contact time (of 24 h), is reported in Fig. 8.

At the equilibrium time, the adsorption capacity increased from 9.60 to 23.21 mg/g with the decrease of PAC dose in membrane from 0.5 to 0.1 g. This can be explained by the split in the flux or the concentration gradient between the solute concentration in the solution and the solute concentration in the surface of the adsorbent (Bouchareb et al., 2019).

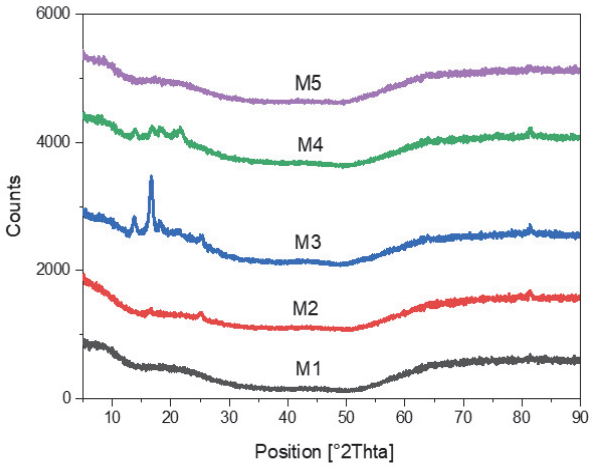

Fig. 5. XRD patterns of CA/PVP/PAC composites membranes

3.3.2. Effect of the initial concentration

The kinetic adsorption of phenol from different initial concentrations for 0.1 g adsorbent dose in membrane is shown in Fig. 9. It can be observed that an increase in the concentration from 5 to 40 mg/L leads to an increase in the adsorption capacity of phenol from 19 to 65 mg/g. This phenomenon can be explained by the fact that the driving force increases with increasing initial concentration (Hamane et al., 2015).

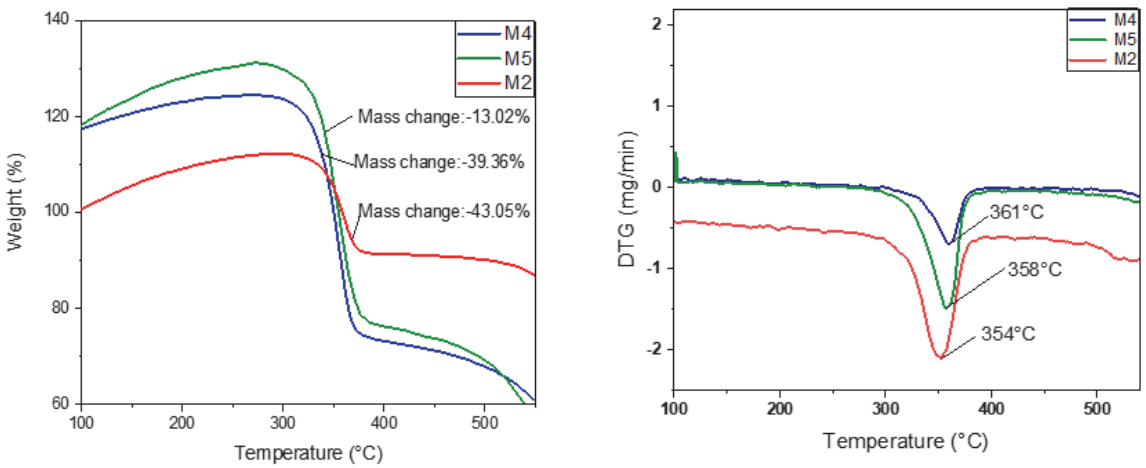

(a) (b)

Fig. 6. Thermogravimetric analysis curves of CA/PVP/PAC composites membranes: (a) TGA and (b) DTG

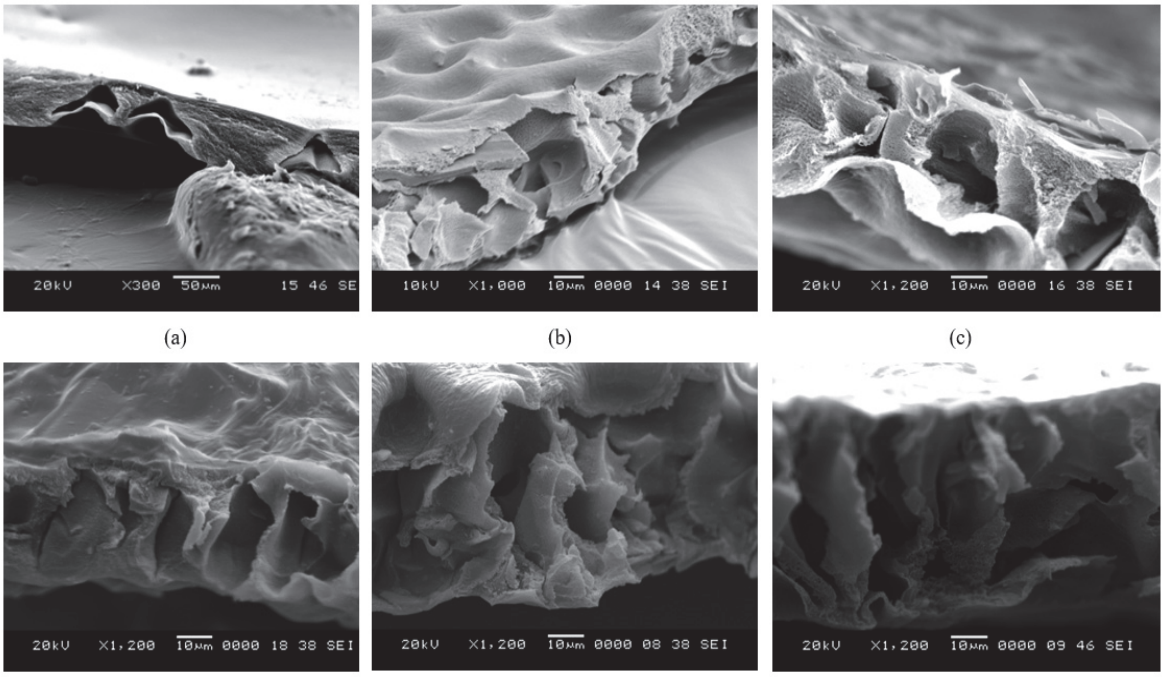

(a) (b) (c)

(d) (e) (f)

Fig. 7. Cross-section SEM images of: (a) CA/PVP membrane (M0) and CA/PVP/PAC composites membranes: (b) M1, (c) M2, (d) M3, (e) M4 and (f) M5

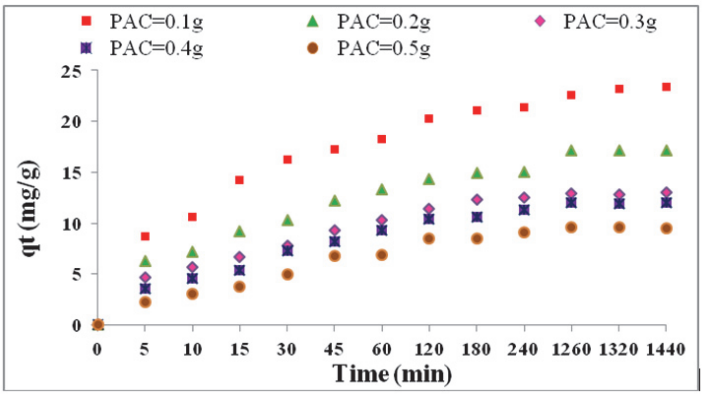

Fig. 8. Effect of adsorbent mass on the adsorption capacity of phenol by CA/PVP/PAC composites membranes (C_0 = 10 mg/L; V= 500 mL; v = 180rpm; ambient temperature; pH = 5.5)

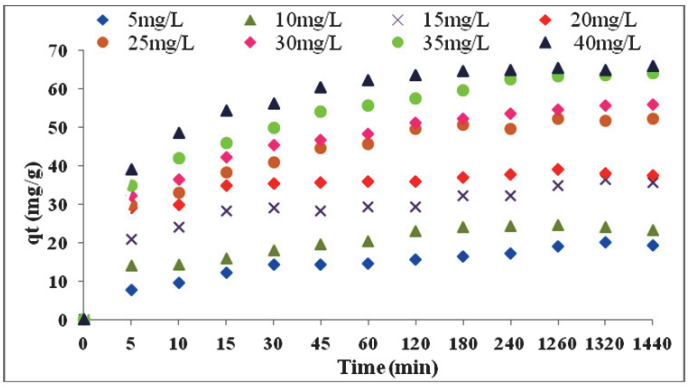

Fig. 9. Effect of initial concentration of phenol on the adsorption capacity by CA/PVP/PAC composites membranes (C_0 = 5-40 mg/L; V = 500 mL; v = 180 rpm; ambient temperature; pH = 5.5; M1)

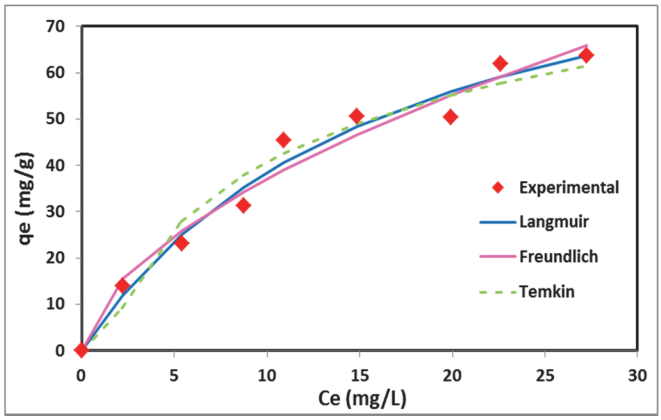

Fig. 10. Effect of pH on the adsorption capacity of phenol by CA/PVP/PAC composites membranes (C_0 = 10 mg/L; V= 500 mL; v = 180rpm; ambient temperature; M1)

3.3.3. Effect of initial pH

The results of the adsorption kinetics of phenol on the CA / PVP / PAC composites membrane for different initial pH values are presented in Fig. 10. The results show that the pH does not have a significant influence on the adsorption capacities for pH 5 and 7. For pH value of 10, the amount of phenol adsorbed at equilibrium is lower. In fact, the adsorption capacity of phenol increases when the pH decreases, that is to say when the amount of the neutral species in solution increases. This can be attributed to the dissociation of phenol which is a function of pH. Phenol, which is a weak acid compound with pKa ≈ 9.89 (Vazquez et al., 2007), is weakly adsorbed at high pH values due to repulsive forces.

At pH> pH_{pzc} of adsorbent (6.15), the adsorbent surface is negatively charged. An electrostatic repulsion occurs between this negative surface and the solute dissociated in the form of phenolate anions, when the pH is greater than the pKa of the solute.

3.4. Isotherms models

Generally, adsorption isotherms offer information on the adsorption capacity, a description of adsorption energy and affinity between the adsorbate and the adsorbent. A number of adsorption equilibrium models have been largely adopted to describe the liquid/solid phase adsorption comportment (El Haouti et al., 2019).

In this study, three broadly used models, Langmuir, Freundlich and Temkin were applied for the fit of the experimental data which are presented in Table 3 (Eqs. 9-11). The fitted isotherms parameters values for non-linear method listed in Table 3, and the model curves are represented in Fig. 11. The equilibrium experimental data for the adsorption of the phenol onto the CA/PVP/PAC composite membrane and the predicted values of the different models shown indicate that the form of the isotherms is L-type according to the classification of Gilles et al. (1960).

Assumption that the adsorbent has a high affinity and there is no competition from the molecules adsorbed into adsorption sites. However, the comparison of the three isotherms models with errors analysis methods indicated higher R^2 and lower χ^2, SSE and RMSE values suggest that the Langmuir isotherm provides adequate fit to the isotherm data which apply a monolayer adsorption for the adsorbent. The maximum adsorption capacity, q_m was found to be 103.08 mg/g. The dimensionless separation factor (R_L) which is the essential characteristic of Langmuir

isotherm is expressed as equation (Eq. 8) (El Haouti et al., 2019):

$$R_L = \frac{1}{(1 + k_L C_0)} \quad (8)$$

where: C_0 is the initial concentration of phenol in solution (mg/L). The value of R_L defines the nature of adsorption.

The value of R_L indicates the isotherm shape to be either unfavourable (R_L>1), linear (R_L=1), favourable (0 < R_L< 1), or irreversible (R_L = 0). The value of dimensionless equilibrium parameter (R_L) was in the range of 0.102-0.054 demonstrating a favourable (0<R_L<1) phenol adsorption on the PAC/CA/PVP composite membrane. The magnitude of the exponent, *1/n*, gives an indication of the favorability of adsorption. The *n* values lie mostly in the range of (1–10), indicating favorable adsorption (Liu et al., 2010; Nekouei et al., 2015).

Therefore the material used has a good affinity with phenol (n > 1). Further, the high value of K_F = 9.83 indicates a high adsorption capacity. Moreover, the Temkin isotherm was studied to explore the Gibbs free energy change as: B = RT/ ΔG° the value of ΔG° was 0.47 kJ/mol, (ΔG°<10 kJ/mol) indicates a physical adsorption process (Hank et al., 2014; Sid-Sahtout et al., 2020). By way of comparison, Table 4 indicates the adsorption of phenol on various composites adsorbents from the literature.

3.5. Adsorption of phenol on the composite membrane in a dialysis treatment

3.5.1. Effect of adsorbent mass

The effect of adsorbent dosage on adsorption of phenol onto CA/PVP/PAC composites membranes is illustrated in Fig. 12.The amount of phenol adsorbed per unit mass of adsorbent decreases with an increase in sorbent dose. This growth in adsorbent dose at constant phenol concentration and volume will lead to unsaturation of adsorption sites through the adsorption process. Moreover, the amount of phenol adsorbed decreases and assigned to overlapping or aggregation of adsorption sites ensuing in a decrease in the total adsorbent surface area available to phenol molecules and an increase in diffusion path length (Guechi and Hamdaoui, 2016).

3.5.2. Effect of the initial concentration on adsorption efficiency

The effect of initial concentration phenol on the adsorption with 0.3 g adsorbent dose is shown in Fig. 13. The amount of phenol adsorbed at equilibrium increased with the initial concentration intensification from 5 to 20 mg /L. This increase may be attributed to the driving force of the concentration gradient (Hamane et al., 2015). Since the resistance to the phenol uptake reduced as the mass transfer driving force increased.

3.5.3. Effect of agitation speed on adsorption efficiency

Fig. 14 shows the adsorption of phenol by PAC-membrane at different stirring speed, ranging from 250 to 450 rpm. The obtained results indicated that the high adsorption capacity was obtained at a low stirring speed of 250 rpm. This agitation speed assures a well diffusion of phenol solute toward adsorbent particles (Guechi and Hamdaoui, 2016). On the other hand, for a high stirring speed of 450 rpm, a substantial reduction of adsorption was observed.

3.6. Response surface methodology (RSM)

Experimental designs are techniques that quantify the effects of various factors on a response to optimize them in specific experimental domains. At first, the factorial design was used in which the statistic results presented an invalidity of the model. So, the response surface methodology was employed in the optimization study.

A central composite design was performed to evaluate the significance of three factors: the amount of adsorbent (X_1), the stirring speed (X_2), and the initial phenol concentration (X_3) on the response (Y), which is the adsorption capacity at equilibrium time (q_e). The levels and ranges of these factors are presented in Table 5. The design was performed in 16 experiments (8 experiments as the full design portion, 6 experiments as the start-points, and two experiments as the center points). The results of the central composite design (Table 6) were analyzed and interpreted using JMP8, by the determination of coefficient R^2 and $R^2_{adjusted}$, the Student's test to evaluate the significance of the regression coefficients, and analysis of variance (ANOVA), for validation of adjusted model (Lazli et al., 2015).

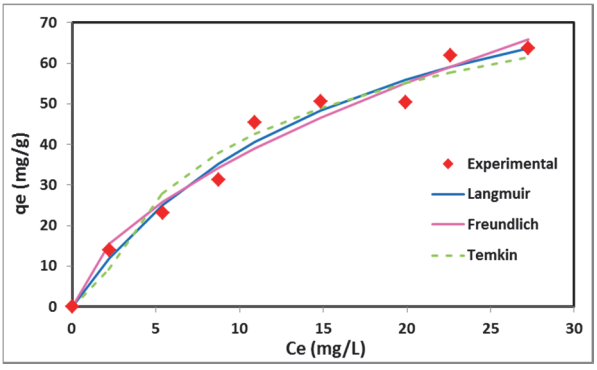

Fig. 11. Isotherms obtained using the non -linear method for the composite membrane CA/ PVP/ PAC (C_0 = 5-40 mg/L; V= 500 mL; v = 180rpm; ambient temperature; pH = 5.5; M1)

Table 3. Isotherm parameters obtained by using non-linear method

Models	*Constants*	*Membrane-PAC*
Langmuir $q_e = \frac{(q_m k_L C_e)}{(1+k_L C_e)}$ (9)	q_m (mg/g)	103.08
	K_L (L/mg)	0.06
	R_L	0.771-0.296
	R^2	0.961
	RMSE	3.6
	SSE	90.522
	χ^2	2.314
Freundlich $q_e = k_F C_e^{1/n}$ (10)	K_f (mg/g). (L/mg)$^{1/n}$	9.83
	1/n	0.58
	n	1.74
	R^2	0.949
	RMSE	4.01
	SSE	112.544
	χ^2	2.675
Temkin $q_e = B_T \ln(k_T C_e)$ (11) $B_T = \frac{RT}{\Delta G^\circ}$	K_t (L/mol)	0.71
	B	20.80
	ΔG° (kJ/mol)	0.12
	R^2	0.936
	RMSE	4.56
	SSE	145.325
	χ2	5.484

Table 4. Comparison of maximum phenol adsorption capacity obtained in this study with previous data

Adsorbents	*Maximum adsorption capacities (mg/g)*	*References*
PAC/CA/PVP composites membranes	103.08	This study
PAC/CA/PVP composites membranes in a dialysis treatment	4.39	This study
Alginate-PAC beads	146.39	Bouchareb et al., 2019
Modified scoria stone	67.11	Sharafi et al., 2019
Activated coal	1.481	Vazquez et al., 2007
Carbonaceous	25.6	Gupta et al., 2016
Fe_3O_4/chitosan/ZIF-8 nanocomposite	6.43	Keshvardoostchokami et al., 2021

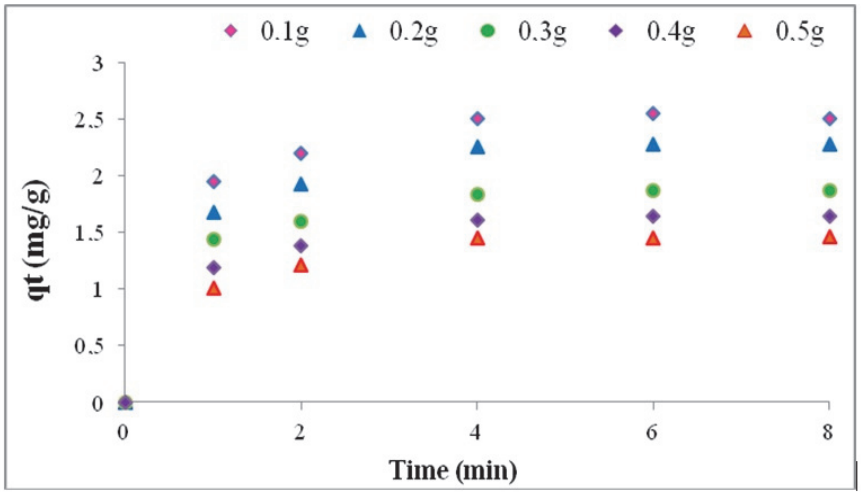

Fig. 12. Effect of adsorbent mass on the adsorption capacity of phenol by CA/PVP/PAC composites membranes in a filtration of dialysis (C_0 = 10 mg/L; V = 250 mL for each compartment; v = 350 rpm; ambient temperature)

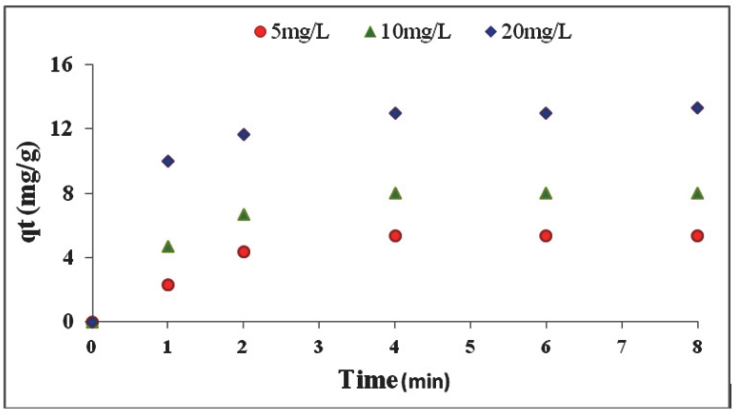

Fig. 13. Effect of initial concentration of phenol on the adsorption capacity by CA/PVP/PAC composites membranes in a filtration of dialysis (C_0 = (5-20) mg/L; V= 250 mL for each compartment; v = 350 rpm; ambient temperature; M3)

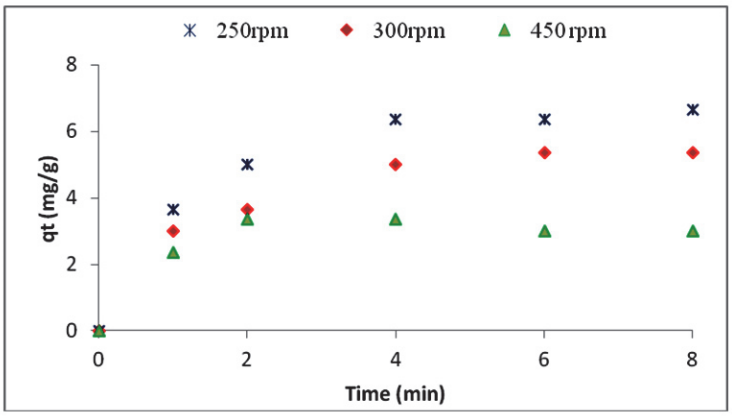

Fig. 14. Effect of agitation speed on the adsorption capacity by CA/PVP/PAC composites membranes in a filtration of dialysis (C_0 = 10 mg/L; V= 250 mL for each compartment; ambient temperature, M3)

Table 5. Domain of variation of the studied factors.

Variables, unit	*Factors*	*Levels*		
		-1	0	1
The mass of adsorbent (g)	X_1	0.1	0.2	0.3
The stirring speed	X_2	250	350	450
Initial phenol concentration (mg/L)	X_3	5	15	25

Table 6. Central composite design and experimental response values

Run	*Factor variables*			*Response*
	X_1	X_2	X_3	q_e *(mg/g) observed value*
1	-1	-1	-1	0.61
2	1	-1	-1	0.90
3	0	0	-1	0.45
4	-1	1	-1	0.45
5	1	1	-1	0.55
6	0	-1	0	1.27
7	-1	0	0	1.64
8	0	0	0	0.90
9	0	0	0	0.98
10	1	0	0	0.75
11	0	1	0	0.75
12	-1	-1	1	4.66
13	1	-1	1	1.60
14	0	0	1	1.20
15	-1	1	1	4.21
16	1	1	1	1.05

The coded mathematical model for the second-order polynomial is given by Eq. (12):

$$Y = a_0 + a_1X_1 + a_2X_2 + a_3X_3 + a_{12}X_1X_2 + a_{13}X_1X_3 + a_{23}X_2X_3 + a_{11}X_1^2 + a_{22}X_2^2 + a_{33}X_3^2 + a_{123}X_1X_2X_3 \quad (12)$$

where: Y is the estimated response, a_0 is the constant, a_i is the linear effect, a_{ii} and a_{ij} represent the squared effect and interactions (Ghaedi et al., 2016), respectively.

By substituting the regression coefficients in Eq. (13) by their numerical values as given in Table 7 we get:

$$Y = 0.7734 - 0.6720X_1 - 0.2030X_2 + 0.9760X_3 - 0.0363X_1X_2 - 0.8263X_1X_3 - 0.0613X_2X_3 + 0.5048X_1^2 + 0.3198X_2^2 + 0.1348X_3^2 + 0.0113X_1X_2X_3 \quad (13)$$

Table 7. Estimated regression coefficients for the adsorption capacity of phenol

Term	*Estimate*	*Standard error*	*T-value*	*P-value*
Constant	0.7734	0.2264	3.4200	0.0189*
X1	-0.6720	0.1512	-4.4400	0.0067*
X2	-0.2030	0.1512	-1.3400	0.2372
X3	0.9760	0.1512	6.4500	0.0013*
X1*X2	-0.0363	0.1693	-0.2100	0.8387
X1*X3	-0.8263	0.1693	-4.8900	0.0045*
X2*X3	-0.0613	0.1693	-0.3600	0.7320
X1*X1	0.5048	0.2946	1.7100	0.1472
X2*X2	0.3198	0.2946	1.0900	0.3271
X3*X3	0.1348	0.2946	0.4600	0.6663
X1*X2*X3	0.0113	0.1691	0.0700	0.9495

Note: An asterisk (*) placed next to p-value it means that the coefficient is significant (P < 0.05)

Fig. 15 shows the predicted values versus the experimental values of the adsorption capacity in equilibrium time, the high value of R^2 = 94.74% and $R^2_{adjusted}$ = 91.24%, fitting the statistical model quite well in correlating the response to the studied parameters (Harfouchi et al., 2016).

3.6.1. Student's t-test

The student's t-test was utilized to determine the significance of the regression coefficients of the parameters. The model terms with P-value should be less than or equal to 0.05 for the effect to be considered statistically significant (Dil et al., 2016; Rosly et al., 2019). After the elimination the no-significant coefficients by one method, the final empirical model for the equilibrium capacity adsorption becomes in Eq. (14).

Based on the sign of each linear effect, the initial concentration of phenol (*X3*) has a positive effect on the equilibrium adsorption capacity, while the mass of adsorbent (*X1*) and the stirring speed (*X2*) have a negative effect.

3.6.2. Interaction plots

The interaction profiler shown in Fig. 16 indicates the effect of one factor at the high and low levels of another factor. The most significant interaction is between initial concentration of phenol and the mass of absorbent (X_1X_3) with a negative value.

$$Y = 0.77 - 0.67X_1 - 0.20X_2 + 0.98X_3 - 0.83X_1X_3 + 0.55X_1^2 + 0.32X_2^2 \quad (14)$$

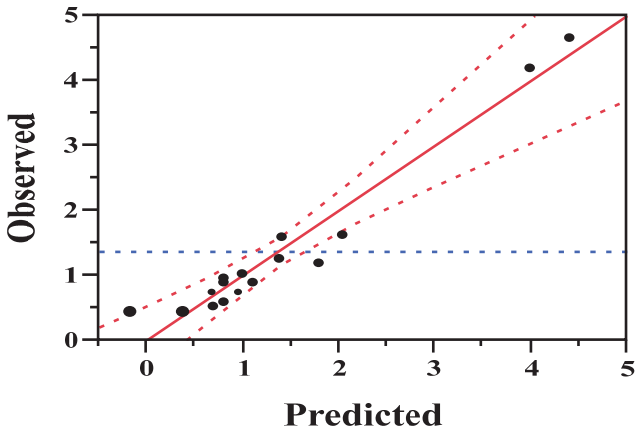

Fig. 15. Observed versus predicted equilibrium adsorption capacity

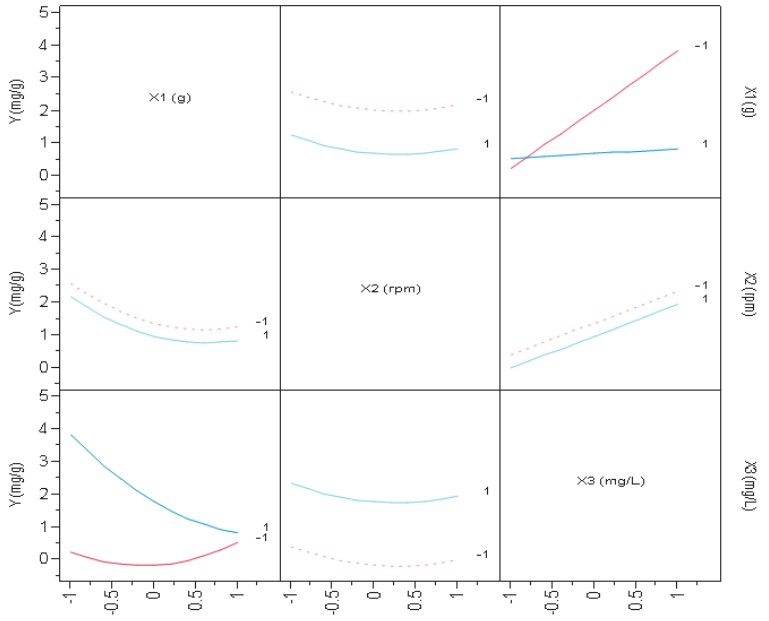

Fig. 16. Interactions plot

Table 8. Analysis of variance

Source	*DF*	*Sum of square*	*Mean square*	*F-value*	*P-value*
Model	6	22.228978	3.70483	27.0389	<0.0001*
Residual	9	1.233166	0.13702		
Total	15	23.462144			
* P < 0.05					

It means that at higher phenol initial concentration, the equilibrium adsorption capacity decreases with the mass of adsorbent. All the other lines of the interaction are parallel, so its effect is not significant.

3.6.3. Analysis of variance (ANOVA)

The performance and significance of the adjusted regression model is analyzed by analysis of variance (ANOVA). The ANOVA results are shown in Table 8. The F-value obtained (27.04) is higher than $F_{0.05,\ 6,\ 9}$ = 3.374 which indicates the validity of the model (Hank et al., 2014).

3.6.4. Estimation of optimal design conditions by the method of desirability function

The desirability function approach is the most current and strongly suggested method to obtain the optimum conditions corresponding to maximum equilibrium adsorption capacity.

According to the prediction profiler in Fig. 17, the maximum adsorbed quantity which equal to 4.39 ± 0.16 mg/g is achieved at the lower levels of the amount of adsorbent (0.1 mg/L) at stirring speed (250) and higher level of initial phenol concentration of 25 mg/L.

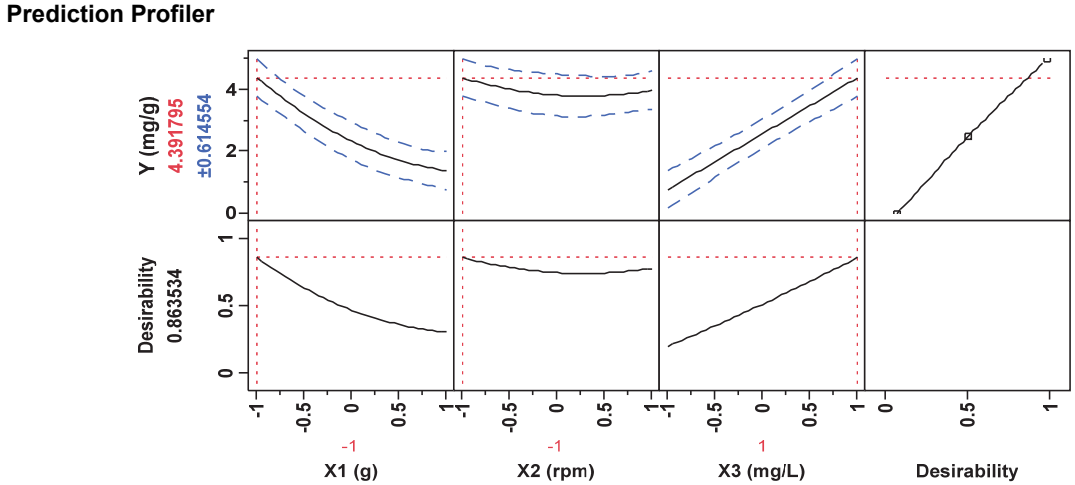

Fig. 17. Desirability functions for response optimization

To confirm optimum response graphically, a spatial representation of the 3D response according to the factors studied is given in the Fig. 18. It is clear that the amount of phenol adsorbed is at maximum when the level of phenol concentration is high and the level of adsorbent mass is low.

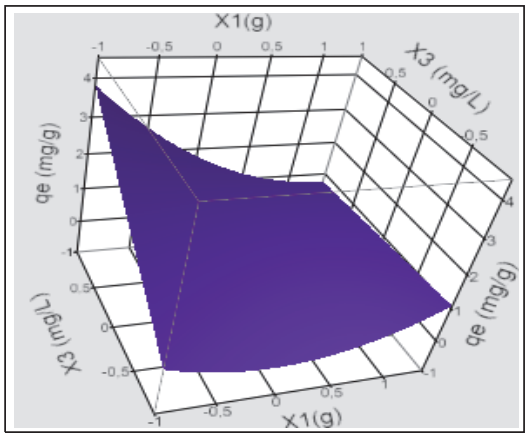

Fig. 18. Response surface 3D showing the effect of adsorbent mass and phenol concentration on phenol adsorption

4. Conclusions

This study has revealed the performance of a new synthesized PAC composite membrane by phase inversion for removal efficiency of phenol from water. The membrane morphologies explored using SEM show that the structure is more porous with more finger-like pores by sponge wall than the structure of non-composite CA membrane, this higher porosity lead to increase the efficiency of the phenol elimination.

In batch system, the adsorption isotherm data fit to Langmuir model. The low value of ΔG°10 KJ/mol signified a physical adsorption process. In a dialysis treatment, the central composite design methodology has been established for predicting and optimizing the adsorption capacity of phenol onto composites membranes.

The model proposed in this study is reasonable and accurate and can be used for predicting the equilibrium adsorption capacity with the limitations of the factors studied. The higher equilibrium adsorption capacity was about 4 mg/g achieved at initial phenol concentrations of 20 mg/L, mass of the PAC 0.1g and slow mixing speed of 250 rpm.

References

Abdellaoui N., Arous O., (2019), Efficient transport of heavy metals across plasticized CTA/PVDF membranes mediated by organo-phosphorous carrier, *Macromolecular Symposia*, **386**, 1-7.

Arthanareeswaran G., Sriyamunadevi T., Raajenthiren M., (2008), Effect of silica particles on cellulose acetate blend ultrafiltration membranes: Part I, *Separation and Purification Technology*, **64**, 38-47.

Arthanareeswaran G., Thanikaivelan P., Srinivasn K., Mohan D., Rajendran M., (2004), Synthesis, characterization and thermal studies on cellulose acetate membranes with additive, *European Polymer Journal*, **40**, 2153-2159.

Ba Mohammed B., Yamni K., Tijani N., Alrashdi A.A., Zouihri H., Dehmani Y., Chung I.M., Kim S.H., Lgaz H., (2019), Adsorptive removal of phenol using faujasite-type Y zeolite: Adsorption isotherms, kinetics and grand canonical Monte Carlo simulation studies, *Journal of Molecular Liquids*, **296**, 1-10.

Belouadah Z., Ati A., Rokbi M., (2015), Characterization of new natural cellulosic fiber from *Lygeum spartum* L., *Carbohydrate Polymers*, **134**, 429-437.

Bensaadi S., Amara M., Arous O., Kerdjoudj H., (2014), Transfer of nitrate ions using a polymeric-surfactant membrane, *Desalination and Water Treatment*, **57**, 1-7.

Bouchareb S., Hank D., Abdel Salam M., Ouddai K., Hellal A., (2019), Adsorption of phenol onto alginate-adsorbent beads prepared from pine cone: equilibrium and factorial design methodology, *Desalination and Water Treatment*, **137**, 143-153.

Cheng L.P., Tai-Horng Young T.H., You W.M., (1998), Formation of crystalline EVAL membranes by controlled mass transfer process in water-DMSO-EVAL copolymer systems, *Journal of Membrane Science*, **145**, 77-90.

Dehkordi F.S., Pakizeh M., Namvar-Mahboub M., (2015), Properties and ultrafiltration efficiency of cellulose acetate/organically modified Mt (CA/OMMt) nanocomposite membrane for humic acid removal, *Applied Clay Science*, **105-106**, 178-185.

Dil E.A., Ghaedi M.,Ghaedi A.M., Asfaram A., Goudarzi A., Hajati S., Soylak M., Agarwal S.,Gupta V.K., (2016), Modeling of quaternary dyes adsorption onto ZnO–NR–AC artificial neural network: Analysis by derivative spectrophotometry, *Journal of Industrial and Engineering Chemistry*, **34**, 186-197.

El Haouti R., Anfar Z., Chennah A., Amaterz E., Zbair M., El Alem N., Benlhachemi A., Ezahri M., (2019), Synthesis of sustainable mesoporous treated fish waste as adsorbent for copper removal, *Groundwater for Sustainable Development*, **8**, 1-9.

Ghaedi M., Khafri H.Z., Asfaram A., Goudarzi A., (2016), Response surface methodology approach for optimization of adsorption of Janus Green B from aqueous solution onto $ZnO/Zn(OH)_2$-NP-AC: Kinetic and isotherm study, *Spectrochimica Acta-Part A: Molecular Biomolecular Spectroscopy*, **152**, 233-240.

Giles C.H., Macewan T.H., Nakhwa S.N., Smith D., (1960), Studies in adsorption. Part XI. A system of classification of solution adsorption isotherms, and its use in diagnosis of adsorption mechanisms and in measurement of specific surface areas of solids, *Journal of the Chemical Society (London)*, **3**, 3973-3993.

Guechi E.K., Hamdaoui O., (2016), Sorption of malachite green from aqueous solution by potato peel: Kinetics and equilibrium modeling using non-linear analysis method, *Arabian Journal of Chemistry*, **9**, S416-S424.

Gupta V.K., Suhas, Tyagi I., Agarwal S., Singh R., Chaudhary M., Harit A., Kushwaha S., (2016), Column operation studies for the removal of dyes and phenols using a low cost adsorbent, *Global Journal of Environmental Science and Management*, **2**, 1-10.

Hamane D., Arous O., Kaouah F., Trari M., Kerdjoudj H., Bendjama Z., (2015), Adsorption/photo-electrodialysis combination system for Pb^{2+} removal using bentonite/membrane/semiconductor, *Journal of Environmental Chemical Engineering*, **3**, 60-69.

Hank D., Azi Z., Ait Hocine S., Chaalal O., Hellal A., (2014), Optimization of phenol adsorption onto bentonite by factorial design methodology, *Journal of Industrial and Engineering Chemistry*, **20**, 2256-2263.

Harfouchi H., Hank D., Hellal A., (2016), Response surface methodology for the elimination of humic substances from water by coagulation using powdered Saddled sea bream scale as coagulant-aid, *Process Safety and Environmental Protection*, **99**, 216-226.

Hassan A.R., Rozali S., Safari N.H.M., Besar B.H., (2018), The roles of polyethersulfone and polyethylene glycol additive on nanofiltration of dyes and membrane morphologies, *Environmental Engineering Research*, **23**, 316-322.

Hwang L.L., Chen J.C., Wey M.Y., (2013), The properties and filtration efficiency of activated carbon polymer composite membranes for the removal of humic acid, *Desalination*, **313**, 166-175.

Hwang L.L., Chen J.C., Wey M.Y., (2014), Effects of membrane compositions and operating conditions on the filtration and backwashing performance of the activated carbon polymer composite membranes, *Desalination*, **352**, 181-189.

Idris A., Yet L.K., (2006), The effect of different molecular weight PEG additives on cellulose acetate asymmetric dialysis membrane performance, *Journal of Membrane Science*, **280**, 920-927.

Karri R.R., Sahu J.N., Jayakumar N.S., (2017), Optimal isotherm parameters for phenol adsorption from aqueous solutions onto coconut shell based activated carbon: Error analysis of linear and non-linear methods, *Journal of the Taiwan Institute of Chemical Engineers*, **80**, 472-487.

Kee C.M., Idris A., (2010), Permeability performance of different molecular weight cellulose acetate hemodialysis membrane, *Separation and Purification Technology*, **75**, 102-113.

Keshvardoostchokami M., Majidi M., Zamani A., Liu B., (2021), Adsorption of phenol on environmentally friendly Fe_3O_4/ chitosan/ zeolitic imidazolate framework-8 nanocomposite: Optimization by experimental design methodology, *Journal of Molecular Liquids*, **323**, 1-10.

Lazli W., Hank D., Zeboudj S., Namane A., Hellal A., (2015), Application of factorial experimental design methodology for the removal of phenol from water by innovate hybrid bioprocess, *Desalination and Water Treatment*, **57**, 6044-6050.

Lin W.J., Shiue G.R., (2011), Elucidation of two water leachable polymers impact on microporous membrane performance and drug permeation, *Journal of Membrane Science*, **373**, 189-195.

Liu Q.S., Zheng T., Wang P., Jiang J.P., Li N., (2010), Adsorption isotherm, kinetic and mechanism studies of some substituted phenols on activated carbon fibers, *Chemical Engineering Journal*, **157**, 348-356.

Mandal A., Das S.K., (2019), Phenol adsorption from wastewater using clarified sludge from basic oxygen furnace, *Journal of Environmental Chemical Engineering*, **7**, 1-8.

Mishra S., Yadav S.S., Rawat S., Singh J., Koduru J.R., (2019), Corn husk derived magnetized activated carbon for the removal of phenol and para-nitrophenol from aqueous solution: Interaction mechanism, insights on adsorbent characteristics, and isothermal, kinetic and thermodynamic properties, *Journal of Environmental Management*, **246**, 362-373.

Mohamad Said K.A.G.G.G., Mohamed Alipah N.A., Ismail N.Z., Jama'in R.L., Mili N., Salleh S.F., Mohamed Amin M.A., Muslimen R., Yakub I., Mohamed Sutan N., (2017), Effect of activated carbon in polysufone-polyethyleneimine-silver composite membrane towards adsorption of chromium (Cr), lead (Pb), silver (Ag) and cadmium (Cd) in synthetic wastewater, *Journal of Materials and Environmental Sciences*, **8**, 3740-3746.

Moradihamedani P., Abdullah A.H., (2017), High-performance cellulose acetate/polysulfone blend ultrafiltration membranes for removal of heavy metals from water, *Water Science and Technology*, **75**, 2422-2433.

Moreno-Castillaa C., Lopez-Ramon M.V., Carrasco-Marın F., (2000), Changes in surface chemistry of activated carbons by wet oxidation, *Carbon*, **38**, 1995-2021.

Mukherjee R., De S., (2016), Novel carbon-nanoparticle polysulfone hollow fiber mixed matrix ultrafiltration membrane: Adsorptive removal of benzene, phenol and toluene from aqueous solution, *Separation and Purification Technology*, **157**, 229-240.

Nadour M., Boukraa F., Benaboura A., (2019), Removal of diclofenac, paracetamol and metronidazole using a carbon-polymeric membrane, *Journal of Environmental Chemical Engineering,* **7**, 1-32.

Nekouei F., Nekouei S., Tyagi I., Gupta V.K., (2015), Kinetic, thermodynamic and isotherm studies for acid blue 129 removal from liquids using copper oxide nanoparticle-modified activated carbon as a novel adsorbent, *Journal of Molecular Liquids*, **201**, 124-133.

Rosly M.B., Jusoh N., Othman N., Rahman H.A., Noah N.F.M., Sulaiman R.N.R., (2019), Effect and optimization parameters of phenol removal in emulsion liquid membrane process via fractional-factorial design, *Chemical Engineering Research and Design*, **145**, 268-278.

Saljoughi E., Mohammadi T., (2009), Cellulose acetate (CA)/polyvinylpyrrolidone (PVP) blend asymmetric membranes: Preparation, morphology and performance, *Desalination*, **249**, 850-854.

Saljoughi E., Sadrzadeh M., Mohammadi T., (2009), Effect of preparation variables on morphology and pure water permeation flux through asymmetric cellulose acetate membranes, *Journal of Membrane Science*, **326**, 627-634.

Sharafi K., Pirsaheb M., Gupta V.K., Agarwal S., Moradi M., Vasseghian Y., Dragoi E.N., (2019), Phenol adsorption on scoria stone as adsorbent: Application of response surface method and artificial neural networks, *Journal of Molecular Liquids*, **274**, 699-714.

Sid-Sahtout N., Hank D., Hellal A., (2020), Characterization and performance of polymer composite membranes for the removal of humic substances from water, *Environmental Engineering and Management Journal*, **19**, 733-746.

Smail F., Arous O., Amara M., Kerdjoudj H., (2013), A competitive transport across polymeric membranes. Study of complexation and separation of ions, *Comptes Rendus Chimie*, **16**, 605-612.

Sun J., Wu L., (2014), Polyether sulfone/hydroxyapatite mixed matrix membranes for protein purification,

Applied Surface Science, **308**, 155-160.

Vazquez I., Rodriguez-Iglesias J., Maranon E., Castrillon L., Alvarez M., (2007), Removal of residual phenols from coke wastewater by adsorption, *Journal of Hazardous Materials*, **147**, 395-400.

Waheed H., Hussain A., (2019), Fabrication of cellulose acetate/polyaziridine blended flat sheet membranes for dialysis application, *BioNanoScience*, **9**, 256-265.

Xuezhong H., (2017), Fabrication of defect-free cellulose acetate hollow fibers by optimization of spinning parameters, *Membranes*, **7**, 27-35.

Zioui D., Arous O., Amara M., Kerdjoudj H., (2011), Polymer inclusion membrane: Effect of the chemical nature of the polymer and plasticizer on the metallic ions transference, *Macromolecules*, **7**, 93-101.

.